A hybrid dielectrophoretic system for trapping of microorganisms from water

Narjes Allahrabbi,[1,2] Yi Shi Michelle Chia,[1] Mohammad S. M. Saifullah,[2] Kian-Meng Lim,[3] and Lin Yue Lanry Yung[1,a)]
[1]*Department of Chemical and Biomolecular Engineering, National University of Singapore, 10 Kent Ridge Crescent, Singapore 119260, Republic of Singapore*
[2]*Institute of Materials Research and Engineering, A*STAR (Agency for Science, Technology and Research), 3 Research Link, Singapore 117602, Republic of Singapore*
[3]*Department of Mechanical Engineering, National University of Singapore, 9 Engineering Drive 1, Singapore 117576, Republic of Singapore*

(Received 20 February 2015; accepted 28 May 2015; published online 15 June 2015)

Assessment of the microbial safety of water resources is among the most critical issues in global water safety. As the current detection methods have limitations such as high cost and long process time, new detection techniques have transpired among which microfluidics is the most attractive alternative. Here, we show a novel hybrid dielectrophoretic (DEP) system to separate and detect two common waterborne pathogens, *Escherichia coli* (*E. coli*), a bacterium, and *Cryptosporidium parvum* (*C. parvum*), a protozoan parasite, from water. The hybrid DEP system integrates a chemical surface coating with a microfluidic device containing inter-digitated microelectrodes to impart positive dielectrophoresis for enhanced trapping of the cells. Trimethoxy(3,3,3-trifluoropropyl) silane, (3-aminopropyl)triethoxysilane, and polydiallyl dimethyl ammonium chloride (p-DADMAC) were used as surface coatings. Static cell adhesion tests showed that among these coatings, the p-DADMAC-coated glass surface provided the most effective cell adhesion for both the pathogens. This was attributed to the positively charged p-DADMAC-coated surface interacting electrostatically with the negatively charged cells suspended in water leading to increased cell trapping efficiency. The trapping efficiency of *E. coli* and *C. parvum* increased from 29.0% and 61.3% in an uncoated DEP system to 51.9% and 82.2% in the hybrid DEP system, respectively. The hybrid system improved the cell trapping by encouraging the formation of cell pearl-chaining. The increment in trapping efficiency in the hybrid DEP system was achieved at an optimal frequency of 1 MHz and voltage of 2.5 V_{pp} for *C. parvum* and 2 V_{pp} for *E. coli*, the latter is lower than 2.5 V_{pp} and 7 V_{pp}, respectively, utilized for obtaining similar efficiency in an uncoated DEP system. © *2015 AIP Publishing LLC*.
[http://dx.doi.org/10.1063/1.4922276]

I. INTRODUCTION

Water safety is indubitably a global public health issue. One of the main concerns in water safety is the pollution of water resources by fecal originated microorganisms.[1] In the aspect of assessing microbial safety of water resources, fecal coliform bacterium such as *Escherichia coli* (*E. coli*) and protozoan parasite such as *Cryptosporidium parvum* (*C. parvum*) are two of the most commonly used indicators to determine the quality of drinking water.[2] Current pathogen detection using culture dependent methods and immunoassay-based techniques are time consuming and expensive. Furthermore, the trend in miniaturization has generated greater efforts in microfluidic separation techniques, as they have numerous advantages such as reducing the

a)Author to whom correspondence should be addressed. Electronic mail: cheyly@nus.edu.sg.

analysis time and less consumption of sample/reagent in addition to portability.[3] Dielectrophoresis (DEP) is among the most utilized microfluidic methods for cell detection, separation, and sorting. DEP phenomenon involves exerting non-uniform electric field (usually generated by an AC current) on cells and is capable of separating unlabeled cells at even rare concentrations.[4] Apart from performing the cell manipulation in label-free manner, DEP has potential to substitute well-known cell separation methods such as centrifugation, filtration, and fluorescent- and magnetically activated cell sorting.

There are various DEP-based methods reported in literature to detect and remove *E. coli* and *C. parvum* from water, such as insulating-based DEP (iDEP) that has the drawback of non-continuous processing of samples.[5–7] This method can possibly lead to disturbed cell capture owing to electrothermal rotation as well as bubble generation attributable to joule heating, both as the result of application of high DC voltage.[8] In addition, iDEP methods, as well as continuous DEP trapping approaches[9–12] and even electrophoresis-based cell separation system,[13] cannot deal with constraint of varying conductivity (i.e., varying ionic strength and pH) of water samples faced in the real-world applications.[8,14]

The DEP performance in providing a selective detection and trapping of the microorganism in water medium can be enhanced by the utilization of surface chemistry to alter the wettability and properties of the microchannels. The use of surface chemistry can aid in achieving better adhesion of the biomolecules to the microchannel surfaces. There is a notable challenge to sustain satisfactory physical interaction between the bioparticles, such as cells, and surfaces to support proper binding.[15] One of the common methods of surface modification to enhance cell adhesion is immuno-assisted surface coating, i.e., the use of immobilized antibodies to trap targeted cells.[16,17] Although this method is selective, it is laborious, time-consuming, expensive owing to the high cost of antibodies, and lack of proper orientations of antibodies for the effective binding of cells. Besides, this method yields low trapping efficiency of cells, e.g., as low as 0.01% to 16% for *E. coli* due to slow diffusion of cells toward immobilized antibodies.[18] Using DEP can enhance the immune capturing of targeted bacterial cells significantly including *E. coli*, *Listeria monocytogenes*, and *Salmonella*.[16] However, it has the same shortfalls on the cost and the antibody orientation. In addition, they are not suitable for the application of trapping multiple cells present in one sample suspension such as a biologically contaminated water sample due to the antibody specificity. Despite having the same shortfall, the DEP enhanced immune capturing and separation of mammalian cells has been reported for circulating tumor cells[19–21] and leucocytes,[22] where both negative DEP (n-DEP) and positive DEP (p-DEP) were used to prevent or promote the capture of the target cells at specific frequencies.

The other well-known surface modification to improve cell adhesion is chemical coating surfaces with silane-bearing compounds and polyelectrolytes. It can result in a highly adhesive surface, effective in cell capturing *via* non-specific binding due to changes in surface wettability or surface charge.[23,24] Such surface modifications are not only inexpensive but also readily available and can be used to trap different types of cells. In a study by van der Mei *et al.*, surface coating using polydiallyl dimethyl ammonium chloride (p-DADMAC) yielded a positively charged surface with improved the cell adhesion of three waterborne microorganisms including *E. coli*.[23] In addition, Dai *et al.* explored the adhesion of *C. parvum* to (3-aminopropyl)triethoxysilane (APTES), fluorosilane and cationic polymer (p-DADMAC) coated particles, and found that the adhesion of negatively charged *C. parvum* onto surfaces is dominated by the electrostatic interactions compared with the hydrophobic interactions.[24] In a flow-based microfluidic system, the possibility of cells flowing at high velocity to contact the antibodies at the precise orientation is low for cell-antibody interaction to occur. However, with a proper chemical coating, cells do not require to surface contact at the specific orientation for the adhesion to occur, since the adhesion is governed by the overall cell surface charge.

Here, we introduce a novel hybrid system that couples the chemically modified surface with DEP-induced cell trapping to continuously trap and detect water-borne pathogens. The hybrid system contains a microfluidic device with inter-digitated microelectrodes imparting p-DEP to enhance the trapping efficiency of continuously flowing cells through the use of the adhesive surface coating. The advantage with the hybrid system is that the fabrication of

microfluidic channel is simple, and it works in the continuous mode as opposed to iDEP methods. In addition, not being purely DEP dependent, the application of hybrid DEP system is not confined by the various conductivity of water samples in the real world. The reason for it is that our system incorporates the robustness of DEP force and cell trapping owing to physical adhesion of cells to the coated microchannel surface. Furthermore, as the cell adhesion occurs in a flow-through microfluidic system, the trapping is not limited by mass-transfer seen in the batch systems.[25] In this work, two well-known waterborne pathogens, *viz*., *C. parvum*, a protozoan, and *E. coli*, a bacterium, were selected. Two silane-bearing agents, trimethoxy (3,3,3-trifluoropropyl) silane (TriF) and APTES, and p-DADMAC, a cationic polyelectrolyte and a flocculant, were used for surface coating.[23] The effectiveness of these coatings was investigated through the static cell adhesion experiments. Then, DEP characterization of cells suspended in water was performed to obtain the optimal operating frequency and minimum required voltage. Finally, using the most effective surface coating and at the optimal frequency, the trapping efficiency of cells in the hybrid DEP system was studied. The low enough voltage was chosen to demonstrate the capability of hybrid system and this was compared with the uncoated DEP system.

II. THEORY

DEP is the motion of particles due to the net force exerted by the non-uniform electric field. The DEP force experienced by a spherical particle (with the volume of *vol*, a relative permittivity of ε_p, and an electrical conductivity of σ_p) suspended in a medium (with a relative permittivity of ε_m, and an electrical conductivity of σ_m) is given by the mathematical equation[4]

$$F_{DEP} = \frac{3}{2}(vol)\,\varepsilon_0\,\varepsilon_m\,Re(f_{CM})\nabla|E|^2, \tag{1}$$

where ε_0 is the permittivity of the vacuum, E is the amplitude of the electric field while $\nabla|E|^2$ is the gradient of electric field squared, and ω (equal to $2\pi f$) is the angular frequency while f is the frequency. For a biological cell more polarizable than its suspending medium, its complex permittivity is bigger than that of the medium. Consequently, $Re(f_{CM})$, real part of the Clausius-Mossotti factor (f_{CM}), is positive and cell is pushed toward the electric field maxima. In this case, the cell is experiencing the p-DEP which usually is the case at the low medium conductivities. For the cell less polarizable than its suspending medium, its complex permittivity is smaller than medium's complex permittivity. Therefore, $Re(f_{CM})$ is negative and cell is pushed toward the region of electric field minima. In this case, the cell is under the n-DEP. The Clausius-Mossotti factor is given by

$$f_{CM} = \frac{\varepsilon_p^* - \varepsilon_m^*}{\varepsilon_p^* + 2\varepsilon_m^*}, \tag{2}$$

where $\varepsilon_p^* = \varepsilon_0\varepsilon_p - j\,\frac{\sigma_p}{\omega}$ and $\varepsilon_m^* = \varepsilon_0\varepsilon_m - j\,\frac{\sigma_m}{\omega}$. $Re(f_{CM})$ is usually between -0.5 and 1.

The DEP force in x-direction can be determined for a cell with the known volume, $Re(f_{CM})$ and the electric field gradient with respect to x-direction. The gradient of electric field squared for the inter-digitated microelectrodes located at the bottom of microchannel is calculated using a commercial finite element package (COMSOL Multiphysics®). According to Eqs. (1) and (2), DEP force is influenced by both the applied frequency and the voltage (to generate the electric field) as well as $Re(f_{CM})$ (an indication of the relative polarizability of the particles compared to the medium). Since cells have the different compartments with the different relative permittivities and the electrical conductivities, an effective f_{CM} is applicable for a single cell. The *C. parvum* and *E. coli* cells can be modeled as a sphere (with radius r) and a prolate ellipsoid (with long semi-axis a and short semi-axis $b = c$), respectively.

In addition to DEP force, a flowing particle in a microchannel also experiences other forces such as the drag force (F_d), the gravitational and the buoyancy forces (F_g and F_b) as shown in

Fig. 1(a). However, the gravitational and the buoyancy forces are considered to be negligible as compared to the DEP force when the cell is small. A flowing particle through the microchannels experiences a drag force, F_d, which is dependent on the flow regime. In microfluidics, the flow is laminar and has a low Reynolds number less than 1.[26] Thus, the drag force (F_d) is calculated by

$$F_d = -6\pi f_1 f_2 \, \mu \, l \, (u_p - u_f), \tag{3}$$

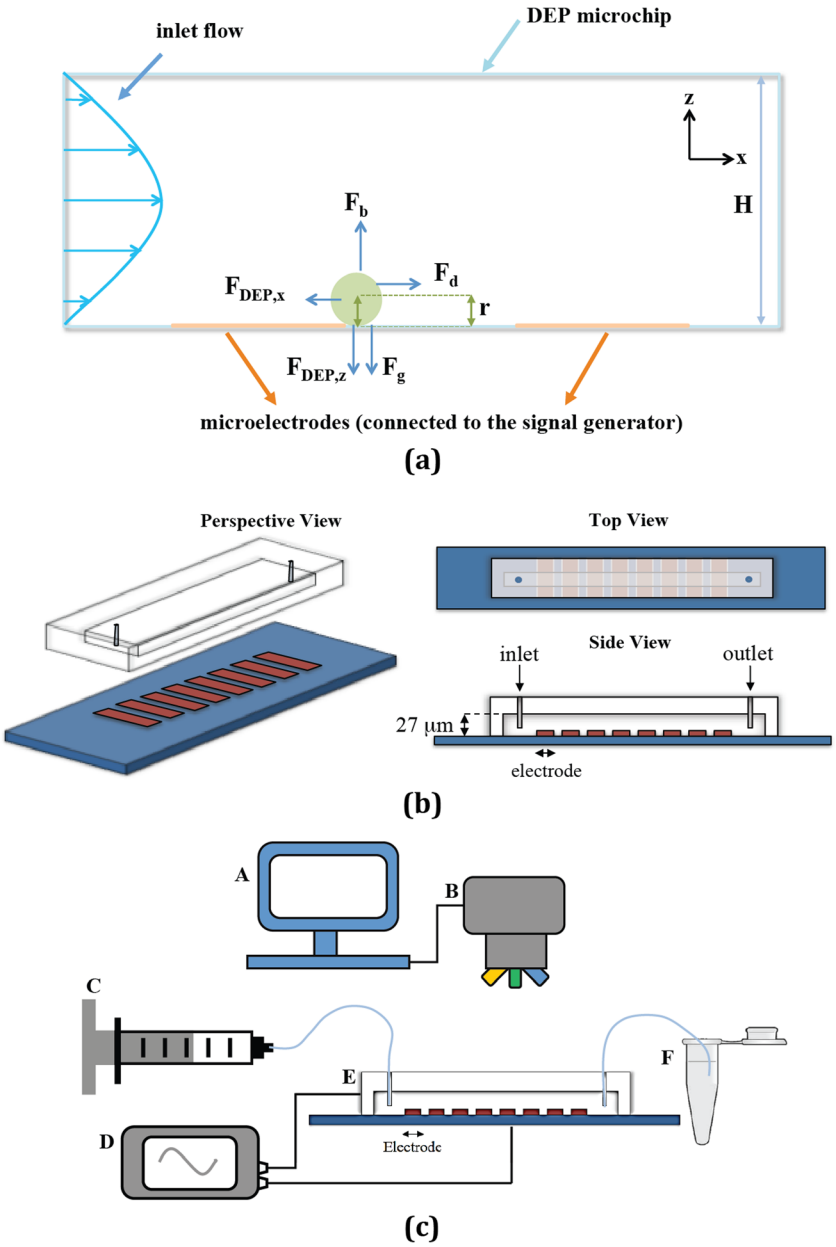

FIG. 1. (a) Schematic diagram showing different forces exerted on a cell in p-DEP flow system. $F_{DEP,X}$, DEP force in the x-direction; $F_{DEP,Z}$, DEP force in the z-direction; F_d, drag force; F_g, gravity force; F_b, buoyancy force; r, cell radius; and H: microchannel height. (b) Schematic drawing of microchannel setup with different views: 45° perspective view, top view, and side view of the microfluidic device. The microchannel has the height of 27 μm. (c) DEP integrated microfluidic experimental set-up. A: Computer with software for viewing and controlling of the optical microscope. B: Bright field/fluorescent microscope (Nikon Eclipse Ti). C: Syringe pump (KDS Scientific, USA). D: Function generator (Agilent 33522 A, USA). E: Assembled microfluidic device with inter-digitated microelectrodes and PDMS microchannel. F: Outlet centrifuge tube for collection of cells.

where μ is the medium viscosity and l is the radius for a spherical cell and the short semi axis for a prolate ellipsoidal cell (when the ellipsoidal cell is moving in parallel with its longest axis). u_p is the velocity of the particle and u_f is the local flow velocity. f_1 and f_2 are the correction factors accounting for the near-wall effects and the deviation of the particle from spherical shape (equal to 1 for a spherical cell), respectively[10]

$$f_1 = \frac{\frac{4}{3}\left(\beta^2 - 1\right)}{\frac{\left(2\beta^2 - 1\right)}{\sqrt{\beta^2 - 1}} \ln\left[\beta + \sqrt{\beta^2 - 1}\right] - \beta}, \quad \beta = \mathrm{a/b}, \tag{4}$$

$$f_2 = \frac{\mathrm{b}\left(\mathrm{K} + \mathrm{a}^2/\mathrm{L}_1\right)}{\pi\left[1 - 0.554\left(\frac{\mathrm{b}}{\mathrm{l}}\right) + 0.1092\left(\frac{\mathrm{b}}{\mathrm{l}}\right)^3 - 0.023\left(\frac{\mathrm{b}}{\mathrm{l}}\right)^4\right]}, \tag{5}$$

$$\text{where } K = \int_0^\infty \frac{ds}{\sqrt{(a^2 + s)(b^2 + s)(c^2 + s)}}, \tag{6}$$

$$L_1 = \int_0^\infty \frac{ds}{(a^2 + s)\sqrt{(a^2 + s)(b^2 + s)(c^2 + s)}}, \tag{7}$$

and l is the distance between cell center to channel wall. Since our microchannel also has a large width to height aspect ratio (larger than 100), it is valid to assume that the fluid velocity profile is parabolic in the direction of the microchannel height (z direction) as illustrated in Fig. 1(a). Besides, as the height of the microelectrodes are about 125 nm, it was assumed to be negligible against the microchannel height for the fluid flow calculations. When H, W, and V_{flow} are the channel height, width of the channel, and the volumetric flow rate, respectively, the local parabolic flow velocity of a particle at the height of r from the bottom is[27]

$$u_f = \frac{6r(H - r)}{H^3 W} V_{flow}. \tag{8}$$

For a particle to get trapped by the p-DEP force against the fluid flow force, the DEP force in x-direction ($F_{DEP,x}$) should be greater than the drag force ($F_{DEP,x} > F_d$). As the particle flows in the medium, it can be pulled downwards towards the electrodes (in the y-direction) by positive DEP. When the particle touches the electrode surface, it will stay on the electrode only if the DEP force in the x-direction balances the fluid drag force, also in the x-direction. For a specific cell in a known medium, if the flow rate and the frequency of the electric field are known, there is a critical voltage (release voltage) at which we can assume $F_{DEP,x} = F_d$. Thus, when the critical voltage is measured, $Re(f_{CM})$ can be calculated as[27]

$$Re(f_{CM}) = \frac{4\,\pi f_1 f_2\,\mu\, l\, u_f}{\varepsilon_0\,\varepsilon_m\,(vol)\,\frac{\partial |E|^2}{\partial x}}, \tag{9}$$

where $\frac{\partial |E|^2}{\partial x}$ is proportional to the square of the applied voltage (V measured as the root mean square or $\mathrm{V_{RMS}}$). To measure the critical voltage at a specific frequency, initially particles are captured at a voltage. The minimum voltage required to trap the cells is called as the capture voltage and it is slightly larger than the critical voltage (release voltage) at which $u_p = 0$. The critical voltage (or the release voltage) is the maximum voltage at which by an incremental decrease in voltage, the cell is released from the DEP trap. At this voltage, it is assumed that $\mathrm{F_{DEP,x}}$ is balanced by $\mathrm{F_d}$. Thus, after the measurement of the critical voltages at the different frequencies, $Re(f_{CM})$ can be calculated and plotted against a spectrum of frequencies. In this

plot, the optimal frequency is recognized as the frequency at which $Re(f_{CM})$ is the largest or in other words, the critical voltage is the smallest.

A biological cell is a complex particle and consists different compartments and internal structures (organelles). Since cells have different compartments with the different electrical conductivities and permittivities, an effective complex permittivity ($\varepsilon^*_{\text{eff}}$) is applicable for a single cell. In addition to the heterogenous nature of the biological cells (for the DEP modelling), they may have non-spherical shape such as bacterial cells. A single-shell model is employed to model *C. parvum*, as a spherical cell (encompasses a cytoplasm and a membrane surrounding it). The effective complex permittivity according to a single-spherical shell model, including a cytoplasm (σ_{cyto} and ε_{cyto}) and a cell membrane (σ_{mem} and ε_{mem}) can be estimated as[28]

$$\varepsilon^*_{eff} = \varepsilon^*_{mem} \frac{\left(\frac{r_2}{r_1}\right)^3 + 2\frac{\varepsilon^*_{cyto} - \varepsilon^*_{mem}}{\varepsilon^*_{cyto} - 2\varepsilon^*_{mem}}}{\left(\frac{r_2}{r_1}\right)^3 - \frac{\varepsilon^*_{cyto} - \varepsilon^*_{mem}}{\varepsilon^*_{cyto} + 2\varepsilon^*_{mem}}}, \tag{10}$$

where ε^*_{cyto} and ε^*_{mem} are complex permittivities for the cell cytoplasm and cell membrane, respectively. r_1 and r_2 are the radii of the core (cytoplasm) and the whole cell (including cytoplasm and membrane), respectively. ε^*_{eff} should be replaced with ε^*_p in Eq. (2) to evaluate $Re(f_{CM})$ for *C. parvum*.

E. coli is modelled as a double-shell ellipsoidal cell, as it is rod shape and entails a protecting layer, called as cell wall, in addition to the cytoplasm and the cell membrane. For the non-spherical cells, the dipole moments are different along each semi-axis. To account for different axial polarizations, a term, called as the depolarization factor for each axis (A_{ix}, A_{iy}, A_{iz}), is utilized to calculate the effective complex permittivity for each axis. As there can be a small difference in $Re(f_{CM})$ of the cell in different orientations, the average value of the f_{CM} for each axis is used towards the calculation of $Re(f_{CM})$ of *E. coli* through the following calculations:[29]

$$\varepsilon^*_{1k} = \varepsilon^*_{wall} \frac{\varepsilon^*_{wall} + (\varepsilon^*_{2k} - \varepsilon^*_{wall})(A_{1k} + \lambda_1(1 - A_{0k}))}{\varepsilon^*_{wall} + (\varepsilon^*_{2k} - \varepsilon^*_{wall})(A_{1k} - \lambda_1 A_{0k})},$$

$$\varepsilon^*_{2k} = \varepsilon^*_{mem} \frac{\varepsilon^*_{mem} + (\varepsilon^*_{cyto} - \varepsilon^*_{mem})(A_{2k} + \lambda_2(1 - A_{1k}))}{\varepsilon^*_{mem} + (\varepsilon^*_{2k} - \varepsilon^*_{wall})(A_{2k} - \lambda_2 A_{1k})},$$

$$A_{ix} = \left\{ \frac{q_i}{(q_i^2 - 1)^{\frac{3}{2}}} \ln\left(q_i + (q_i^2 - 1)^{\frac{1}{2}}\right) \right\} - \frac{1}{q_i^2 - 1},$$

$$A_{iy} = A_{iz} = \frac{1}{2}(1 - A_{ix}),$$

where $\lambda_1 = \frac{a_1 b_1 c_1}{a_0 b_0 c_0}$, $\lambda_2 = \frac{a_2 b_2 c_2}{a_1 b_1 c_1}$, and $q_i = \frac{a_i}{b_i}$.
Thus,

$$Re(f_{CM}) = Real\left(\frac{1}{3}\sum_{i=x,y,z} f_{CM_i}\right) = Real\left(\frac{1}{3}\sum_{i=x,y,z}\frac{1}{3}\left(\frac{\varepsilon^*_{1k} - \varepsilon^*_m}{\varepsilon^*_m + (\varepsilon^*_{1k} - \varepsilon^*_m)A_{0k}}\right)\right). \tag{11}$$

III. MATERIALS AND METHODS

A. Fabrication of the microfluidic chip

Patterning of the inter-digitated microelectrodes and the microchannel master mold (replica) were done through photolithography. Indium tin oxide sputtered glass wafers (ITO-glass)

were purchased (Bonda Technology Private Ltd., Singapore). ITO was chosen for electrodes due to its high electrical conductivity and superior transparency to observe the cell behavior under an optical microscope. After washing the ITO-glass wafer with *iso*-propanol, acetone and distilled (DI) water, it was coated with the positive photoresist AZ 2001 (Microchem Corp., USA) *via* spin coating at 1500 rpm for 30 s and baked for 2 min at 95 °C. Next, it was exposed to the ultraviolet (UV) light through the positive mask (IGI, Singapore) using a mask aligner system (Karl Süss MA4 Mask Aligner, USA) at an intensity of about 60 mJ/cm^2. Subsequently, the exposed ITO-glass was immersed in the AZ 400 K developer for 30 s to dissolve away the exposed photoresist. Finally, the ITO-glass was wet etched for about 10 min with 16% (w/v) ferric (III) chloride (anhydrous, Sigma-Aldrich) in the equi-volume mixture of DI water and hydrochloric acid (37%, Sigma-Aldrich) to remove the unprotected regions of the ITO layer on glass wafer. Finally, the photoresist layer was removed through immersing in acetone and rinsed using DI water.

To fabricate the microchannel replica mold (i.e., master mold), silicon wafers were purchased (Bonda Technology Private Ltd., Singapore). After washing the silicon wafer with *iso*-propanol, acetone and DI water, it was coated with the negative photoresist SU-8 3025 (Microchem Corp., USA) at a spin coating speed of 3000 rpm for 30 s and then pre-baked for 10 min at 95 °C. In the next step, it was exposed to the UV light through the negative mask (IGI, Singapore) using the mask aligner system at an intensity of about 60 mJ/cm^2. The exposed silicon wafer was post-baked at 65 °C for 1 min and at 95 °C for 3 min. After this step, it was developed with the SU-8 developer for 45 s. After the final baking at 100 °C for 5 min, the silicon microchannel replica mold was ready for the further use. Polydimethylsiloxane (PDMS) mixture (Sylgard 184 silicone elastomer kit, Dow Corning, USA) was prepared by the addition of PDMS elastomer and curing agent with 10:1 weight ratio and poured on the microchannel replica mold. It was vacuum dried to remove the bubbles trapped in the mixture and then baked in an oven for 2 h at 70 °C. Afterwards, the cast PDMS is peeled off from the replica mold and it cuts in proper size. Finally, the inlet and outlet holes were punched in the PDMS microchannel and UV plasma-treated to bind it to the ITO-glass. The final channel was about 20 mm long, 3 mm wide, and 0.027 mm high. The final schematic view of the microchannel is as illustrated in Fig. 1(b).

B. Preparation of cell samples and coated surfaces

C. parvum oocysts, calf sourced, with the population of 5×10^7 in phosphate buffered saline (PBS) was purchased from Waterborne, Inc. (USA). *E. coli UTI89* strain (obtained from Genome of Institute of Singapore, A*STAR) was cultured in the autoclaved Lysogeny broth (LB). An aliquot of *C. parvum* in PBS/*E. coli* in the LB medium was spun down through the centrifugation and was washed twice to remove any excess PBS/ LB medium. Thereafter, the washed pellets were resuspended in DI water to obtain a concentration of about $10^5/10^7$ count per ml which was measured by hemocytometry. Due to the small size of *E. coli* cells, there was a limitation in obtaining the lower concentrations of the cells through measuring by hemocytometry. To stain cells, the green fluorescent nucleic acid stain, Styo9 (Live/Dead® BacLight Viability Kit) was incubated with them. Then, the pellets were spun down and washed, as explained earlier, to remove the excess stain.

The surface coating agents used in this study were: APTES (99% purity, Sigma-Aldrich), TriF (≥97.0% purity, Sigma-Aldrich), and p-DADMAC (20 wt. % in H_2O, Sigma-Aldrich). 1% (v/v) and 5% (v/v) APTES and TriF solutions were prepared by the dissolution of 400 and 2000 μl APTES and TriF, respectively, in 40 ml absolute ethanol. On the other hand, 500 and 1000 ppm p-DADMAC solutions were prepared by adding 104 and 208 mg of 20 wt. % p-DADMAC in 40 ml DI water. The solutions were homogenized by vortexing.

To clean the glass substrates before the static cell adhesion test, they were sequentially immersed in acetone, DI water, and ethanol under sonication each for 15 min. They were air dried and ready for the surface coating of APTES and TriF. For the surface coating of p-DADMAC on glass, the cleaning steps in DI water and ethanol were reversed. The cleaned

glass slides were soaked into the prepared coating solutions for 15, 30, or 60 min. To investigate the effect of the agent concentration, the soaking time was kept at 60 min and the coating agents with two different concentrations were tested. Subsequently, the coated glass slides were washed with DI water to remove any excess coating and air dried. In order to evaluate the outcome of heat curing, the glass slides coated at a lower coating agent concentration (1% for TriF and APTES and 500 ppm for p-DADMAC) were curried overnight (8 h) in an oven at 25 °C and 70 °C. The coated glass slides were then immersed in wells containing 3 ml of the cell suspension for 15 min with the application of the orbital agitation. Next, they were washed with DI water to remove the unbound cells. The number of the adhered cells was counted in the magnification fields of 40*X* (area of 0.00067 cm^2) and 20*X* (area of 0.00291 cm^2) for *E. coli* and *C. parvum,* respectively.

The water contact angle was measured *via* a manual contact angle measurement meter. The measurements were made within 10 to 30 s after a drop of approximately 10 μl of DI water was placed on the surface of the uncoated and the coated glass substrate by a micro-syringe. Three measurements were taken for each sample, and the same sample was prepared twice again independently to obtain a total of 9 measurements.

C. Experiments

1. Determination of the capture and critical voltages

A 1 mm wide microchannel was fixed on the optical microscope stage. The wires linked to the microelectrodes were connected to the electric signal generator. The experimental setup for the conduction of the experiments is schematically shown in Fig. 1(c). The prepared sample of *C. parvum*/*E. coli* cells was pumped into a microchannel by a syringe pump. In the microchannel, the cells are flown perpendicularly at a small flow rate of 50 μl/h (low enough to better observe cell behavior) over the inter-digitated microelectrodes situated at the bottom of the microchannel. Cell behavior was observed *via* the bright field microscope when they were flowing over the first few inter-digitated microelectrodes in the middle of the microchannel. After choosing a specific frequency, the voltage was slowly increased by 0.1 V_{pp} increments until a capture voltage was reached where the first few cells were trapped by the electrodes. Thereafter, the voltage was slowly decreased until the voltage at which the same cells were released from the electrodes. This voltage was recorded as the critical voltage. The capture voltages and the critical voltages (release voltages) were recorded for the different frequencies in the range of 50 kHz to 30 MHz. At each frequency, five capture and five release voltages (or critical voltages) were obtained in three independent experiments using different batches of cultured cells.

2. Experiments with the uncoated DEP system

The prepared water sample of *E. coli*/*C. parvum* cells was pumped into a wider microchannel of 3 mm by a syringe pump. A higher flow rate of 100 μl/h was used to increase the throughput volume per unit time. After setting the frequency and the voltage and switching on the electric field, the system ran for 30 min to collect the outlet cells. The cell concentrations in the inlet and the outlet flow were determined *via* hemocytometry. New PDMS microchannel and tubings were used for every run.

3. Experiments with the hybrid DEP system

The p-DADMAC coating solution was pumped into the microchannel and allowed to react with the surface for 60 min and then cured by heat. Thereafter, the excess surface coating agent was washed out by pumping DI water into the microchannel at a rate of 10 μl/h. After the excess surface coating agent was washed out, the cell suspension was pumped in at a flow rate of 100 μl/h. Similar to the uncoated DEP system, the hybrid DEP system was allowed to operate for 30 min, and the cell concentrations at the inlet and the outlet flow were determined to evaluate the trapping efficiency of the system.

IV. RESULTS AND DISCUSSION

A. Static cell adhesion on the coated glass substrates

Preliminary studies on the static cell adhesion on the coated glass substrates were done to find the effective surface coating agent and coating conditions for enhanced cell adhesion in order to implement it in the hybrid p-DEP system. Molecular structures of three coating agents are illustrated in the supplementary material Fig. SI1.[30] The cell adhesion to the surfaces is generally influenced by the electrostatic and hydrophobic interactions.[24,31–33] The enhanced adhesion of hydrophobic cells/charged cells to the hydrophobic/oppositely charged surfaces can be related back to the hydrophobic/electrostatic interactions.[31] Thus, it is important to investigate the zeta potential (an indication of the cell/surface charge) and water contact angle (an indication of the surface hydrophobicity) of the coated surfaces. Since both *E. coli* and *C. parvum*, when suspended in DI water, have comparable zeta potentials of about −16 mV and −15 mV, respectively, only *E. coli* was selected for static cell adhesion tests. Despite the hydrophobic nature of *C. parvum*,[24] the role of hydrophobic interaction in *E. coli* adhesion is a controversial issue.[32,33] Thus, we chose to perform the static cell adhesion tests with *E. coli* as its greatest affinity towards either the charged or the hydrophobic surface is unclear. For all the three coating agents, the impacts of different coating conditions on the enhancement of the *E. coli* cell adhesion were tested, including: (1) the soaking time between the coating agent and the glass substrate, (2) the coating agent concentration, and (3) the heat curing of the coated substrate. The coating condition was optimized stepwise in order to achieve the maximum *E. coli* adhesion (see in the supplementary material Fig. SI2[30]). The optimal coating condition was chosen as 60 min of soaking time for all coating agents, for the efficacy of soaking time on cell adhesion appears to flatten after 45 min. Therefore, at this coating condition, concentration of the coating agents was 500 ppm for p-DADMAC, 1% (v/v) for APTES and TriF, and overnight curing at 70 °C for both the p-DADMAC and APTES-coated and 25 °C for TriF-coated surfaces.

The water contact angle measurements for the uncoated and the optimally coated surfaces are summarized in Fig. 2(a). Both the APTES and TriF-coated surfaces displayed slightly higher hydrophobicity than p-DADMAC-coated surface. The summary of the static cell adhesion count of *E. coli* to the uncoated and the optimally coated surfaces is shown in Fig. 2(b). Although the three coatings improved *E. coli* adhesion, the p-DADMAC-coated surface was found to be the most effective in enhancing cell adhesion. Previous studies have shown that the measured zeta potential of the p-DADMAC, APTES, and TriF-coated surfaces (in contact with water) were about +60 mV,[24] +7 mV,[34] and −14 mV,[35] respectively. It can be concluded that p-DADMAC highly positive-charged surface (i.e., the electrostatic interaction) played an important role in the enhanced adhesion of *E. coli,* which carried a high negative charge (zeta potential of about −16 mV when suspended in DI water). Studies show that in a low ionic strength medium such as in water, the long-range electrostatic interactions (in this case, the attractive electrostatic force due to the opposite charges on the surface and the cell) have exhibited the dominancy in bacterial adhesion such as *E. coli* adhesion due to the higher zeta potential in the medium (with the lower ionic strength).[32]

The static adhesion tests with the three optimally coated surfaces were also carried out for *C. parvum* (Fig. 2(c)). It can be inferred that p-DADMAC-coated surface proved to be the most effective surface for enhanced *C. parvum* adhesion. Despite *E. coli*'s tendency to adhere to all coated surfaces, *C. parvum* only tended to adhere to the p-DADMAC-coated surface (p-value < 0.05). This is in agreement with the claim of Drozd and Schwartzbrod regarding the negligible hydrophobicity of *C. parvum*[36] and the assertion of Dai *et al.* about the prevailing role of the oppositely charged surface in *C. parvum* adhesion to the surfaces.[24] Dai *et al.* showed that the adhesion of *C. parvum* due to the electrostatic interactions was irreversible, while the adhesion provoked by the hydrophobic interactions can be reversible *via* dilution or washing.[24] This indirectly proposes that the cell adhesion to the hydrophobic surface may be susceptible to change if the ionic strength (i.e., electrical conductivity) of the water sample changes.

In brief, both of *C. parvum* and *E. coli* cells were strongly adhered to the positively charged p-DADMAC-coated surface by means of the electrostatic interactions. Subsequently,

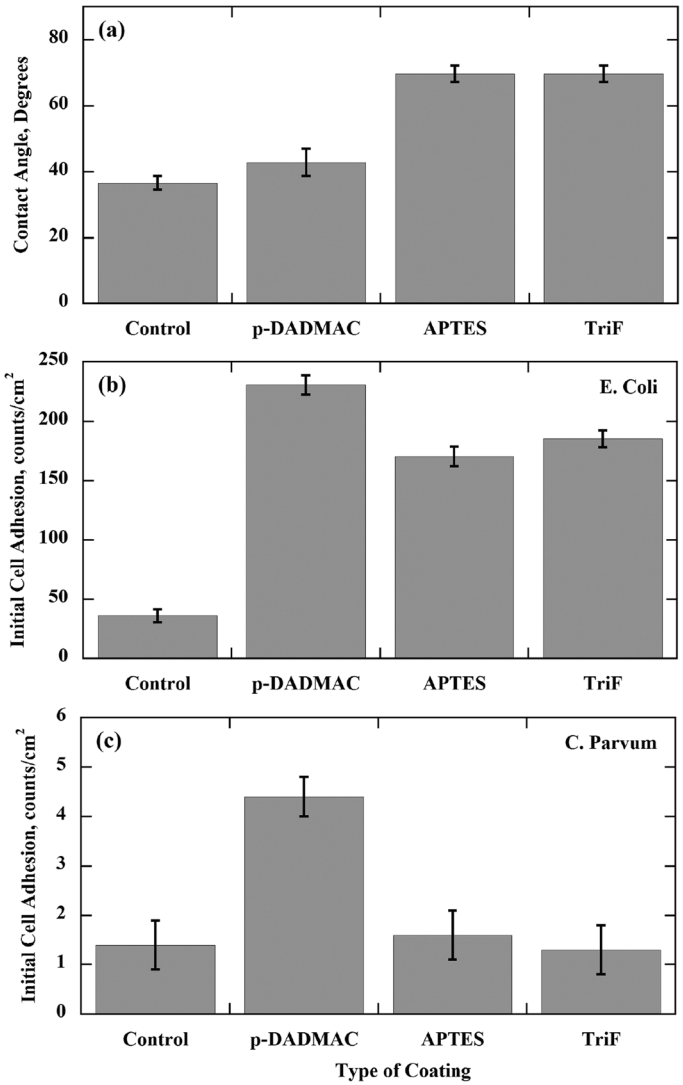

FIG. 2. (a) Water contact angle measurement of the uncoated glass (control) and coated glass. (b) *E. coli* and (c) *C. parvum* adhesion to the uncoated glass (control) and coated glass. The coating parameters are the following: p-DADMAC (soaking time: 60 min, coating concentration: 500 ppm, overnight curing: 70 °C); APTES (soaking time: 60 min, coating concentration: 1% (v/v), curing temperature: 70 °C, 8 h); and TriF (soaking time: 60 min, coating concentration: 1% (v/v), curing temperature: 25 °C, 8 h). The areas used for cell adhesion calculations were 0.00067 cm^2 and 0.00291 cm^2 for *E. coli* and *C. parvum*, respectively.

adhesion of both the cells may tend towards an irreversible binding through the production of specific ligands or proteins.[32,37] Hence, p-DADMAC is the best coating agent to employ for further improvement of the trapping efficiency in the hybrid DEP system.

B. DEP characterization of cells

DEP characterization for both cells was done to determine the optimal condition (i.e., optimal frequency) for applying the p-DEP force on cells. Thus, $Re(f_{CM})$ was plotted against logarithm of frequency to find the optimal frequency. Figs. 3(a) and 3(b) show the recorded capture voltage and the critical voltage (release voltage) for *E. coli* and *C. parvum*, respectively, between the frequency range of 50 kHz to 30 MHz. The critical voltage was employed to calculate $Re(f_{CM})$ by Eq. (9). The parameters used for calculations are listed in Table I. Figs. 3(c) and 3(d) illustrate the calculated $Re(f_{CM})$ in the same spectrum of the frequencies for *E. coli*

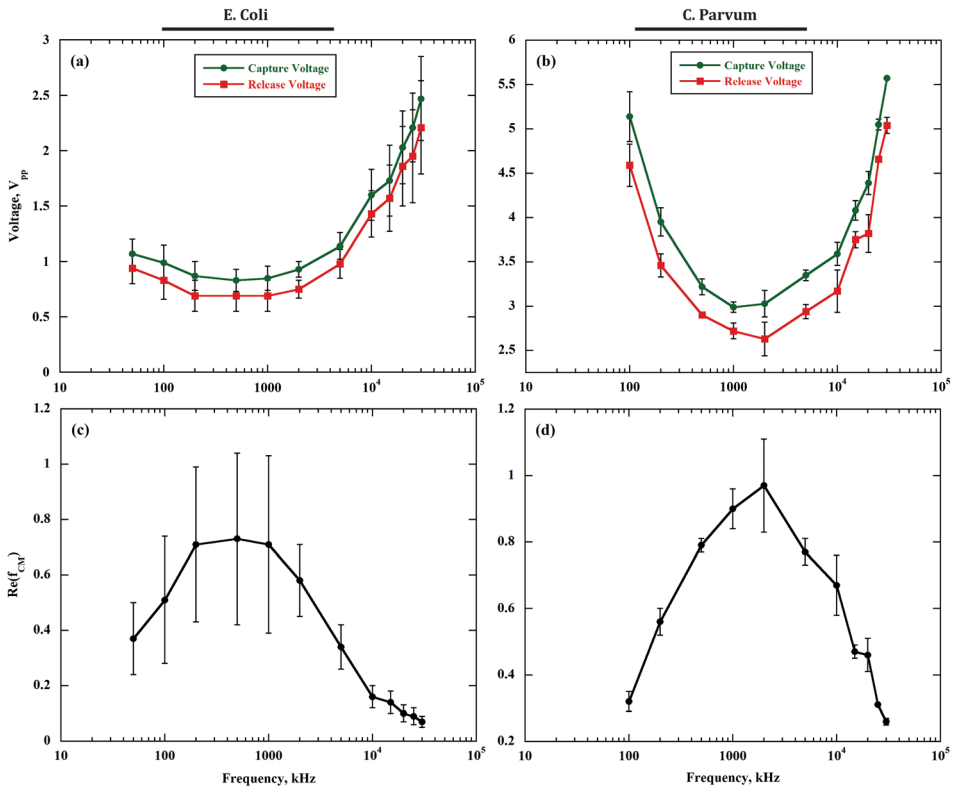

FIG. 3. Capture and release voltage (critical voltage) for (a) *E. coli* and (b) *C. parvum*. Cell characterization curve for (c) *E. coli* and (d) *C. parvum*. The value of $Re(f_{CM})$ used for plotting the graph was calculated using the average critical (release) voltages obtained from the experiment. The parameters used in the calculation are shown in Table I.

and *C. parvum*, respectively. The optimal frequency required for the p-DEP trapping of cells is the frequency with the maximum $Re(f_{CM})$ (i.e., DEP force is the largest). Thus, according to Figs. 3(c) and 3(d), the optimal frequency, respectively, for trapping both *E. coli* and *C. parvum* is about 1 MHz.

Fig. 4 shows $Re(f_{CM})$ for *E. coli* and *C. parvum* cells as compared with the value of $Re(f_{CM})$ calculated using the reported cell properties (permittivity and conductivity) and the water sample conductivity of 1 mS/m for *E. coli*[38] (using Eq. (11)) and *C. parvum*[10] (through Eq. (10)), respectively. The reason for the difference in $Re(f_{CMa})$ for *E. coli* in low and intermediate frequency regions can be due to the different strains of *E. coli* used in these two researches (5k[38] *versus UTI89*). Studies showed that bacterial cells such as *E. coli* with

TABLE I. Parameters used for calculations of $Re(f_{CM})$.

Parameters	*E. coli*	*C. parvum*
ε_0	8.845×10^{12} F/m	
ε_m	78	
μ	0.001 Pa s	
V_{flow}	50 μl/h	
Cell size	$a = 0.85\ \mu$m	$r = 2.3538\ \mu$m
	$b = 0.4\ \mu$m	
Wall correction factor, f_1	8.8443×10^{-1}	1.1962
Shape factor, f_2	1.2294	1.000
$\frac{\delta\lvert E\rvert^2_{V_o=1}}{\delta x}$	1.7328×10^{16}	2.7728×10^{14}

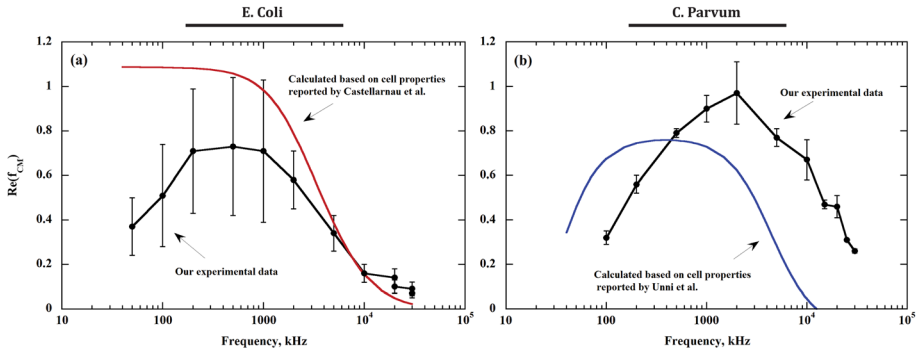

FIG. 4. The value of $Re(f_{CM})$ for *E. coli* (a) and *C. parvum* (b) plotted based on the recorded critical voltage and compared with that calculated using the reported cell properties in the literature.

different strains or serotypes can have relatively different $Re(f_{CM})$.[38–41] The small shift in $Re(f_{CM})$ for *C. parvum* can be attributed to the storage duration and condition of the *C. parvum* samples. Kuhnert-Paul suggested that during the storage of *C. parvum*, the permeability of oocysts can increase relatively fast over time, and their morphology can change depending on the storage temperature and duration.[42] Hence, it can affect the ion content and the electrical properties of the cell, resulting in a slight shift in plot of $Re(f_{CM})$ for *C. parvum*.

In DEP characterization, the low flow rate of 50 μl/h and small 1 mm-wide microchannel were used to facilitate the observation of the cell behavior in the DEP microfluidic system. However, for the subsequent experiments, a 3 mm-wide microchannel was used with an increase in flow rate to 100 μl/h. A wider microchannel provides an increase in the available areas for trapping cells, which are the edges of the microelectrodes (the region of the electric field maxima). In addition, a higher flow rate would mean a higher throughput, and thus reduce the required operation time to process each sample. Hence, by relating back $Re(f_{CM})$ to the critical voltage using the new flow rate, at the same optimal frequency, the new critical voltage was evaluated for *E. coli* and *C. parvum* as 0.74 and 2.42 V_{pp}, respectively, to use as the base voltage to trap the cells. Meanwhile, a higher flow rate was not chosen for the experiments as a higher voltage is required to trap the cells, which can cause the adverse impact on the cell viability (i.e., transmembrane voltage and Joule heating).[43]

C. Performance of the uncoated DEP system

The performance of the DEP system, including the microfluidic channel with the interdigitated microelectrodes, against voltage was evaluated based on the efficiency of the DEP cell trapping. The trapping efficiency can be formalized by equation

$$\text{Trapping Efficiency} = \frac{C_{inlet} - C_{outlet}}{C_{inlet}} \times 100\%, \tag{12}$$

where C_{inlet} is the concentration of cells in the microchannel inlet and C_{outlet} is the concentration of cells in the microchannel outlet.

Figs. 5(a), 5(b), 6(a), and 6(b) demonstrate the improvement of the p-DEP cell trapping as a function of applied voltage in the uncoated DEP system. The applied voltage was incrementally increased starting from the voltage around the critical voltages for *E. coli* and *C. parvum* cells, respectively. These figures clearly indicated the increase in trapping efficiency by an increase in voltage (at the optimal frequency). According to Fig. 5(a), despite the initial outstanding improvement rate in trapping efficiency of *E. coli* cells *versus* the voltage, the rate of improvement of trapping efficiency decreases with the further increase of voltage due to the saturation of inter-electrodes gap. Besides, due to the increased local cell volume fraction at high voltages, the drag force on cells would likely to increase as a result of enhanced apparent viscosity.[44] Thus, this effect may slightly counteract the cell trapping improvement due to

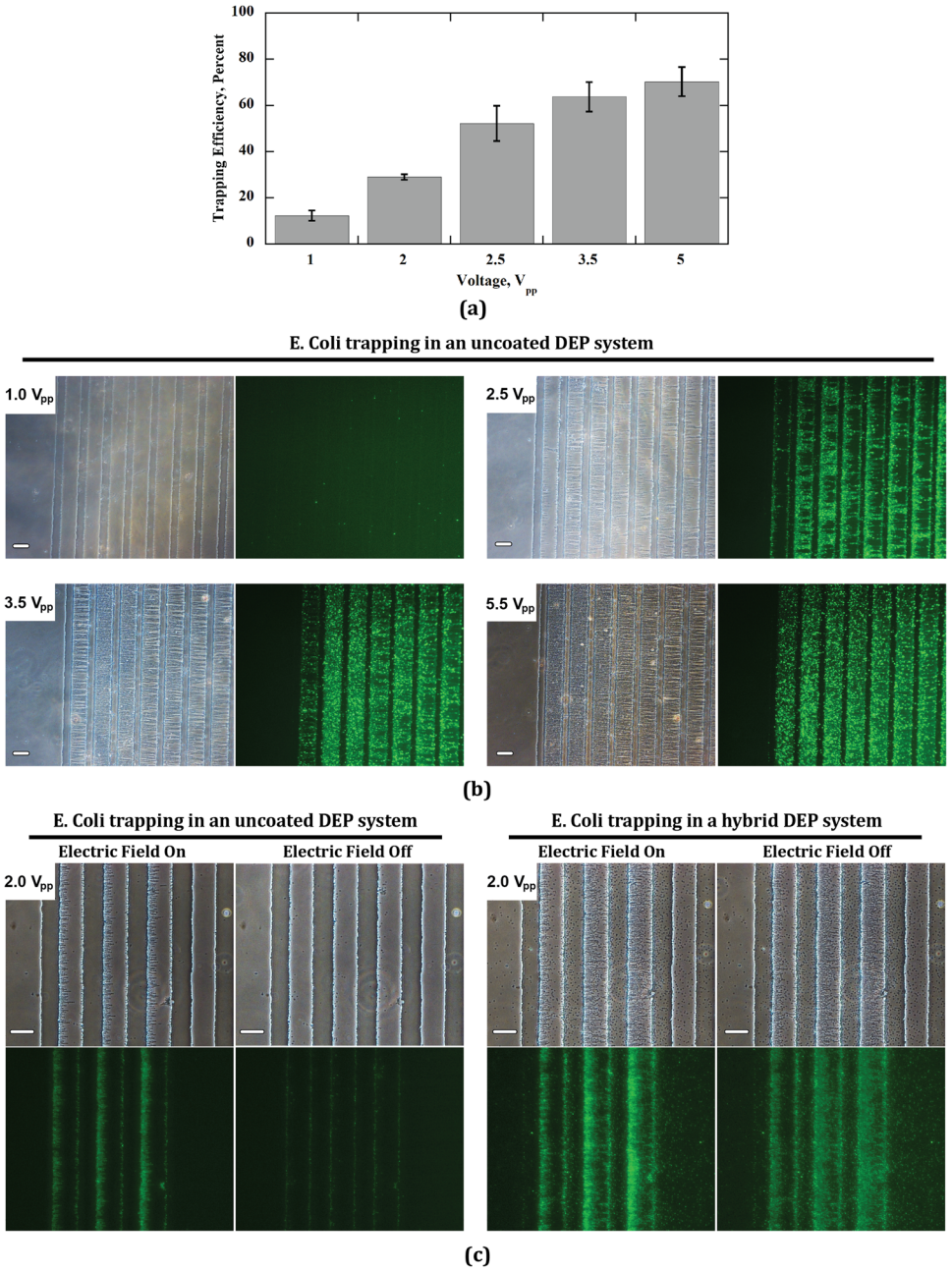

FIG. 5. (a) Change of trapping efficiency for *E. coli* cells with respect to voltage in an uncoated DEP system and (b) its respective fluorescent and optical microscopic images (at $t = 30$ s). (c) Trapping of *E. coli* cells in an uncoated and coated (hybrid) DEP system with electric field on and subsequently turning it off (at $t = 300$ s). Length of scale bars = 30 μm.

pearl-chaining. This can lead to change in the flow field and decrease in electric field on the subsequent incoming cells due to presence of the retained cells that impacts further cell trapping.[45–47] Unlike *E. coli* trapping displayed in Fig. 5(b), saturation of the electrodes was not observed in for *C. parvum* at high voltages (Fig. 6(b)). This could be due to the low number (the low inlet concentration) of *C. parvum* in the suspension. Nonetheless, pearl chaining of *C. parvum* cells was observed similar to *E. coli* at high voltages (2.5 V_{pp}, 4 V_{pp}, and 7 V_{pp}). The pearl chaining of cells, which was due to the interaction of the oppositely charged regions on the cells, in the initial trapping stages, can enhance the trapping of cells rapidly before the

inter-electrode gaps get saturated.[48,49] However, the reduction in the improvement rate in *C. parvum* trapping by increasing voltage from 4 V_{pp} to 7 V_{pp} was similarly observed.

That the trapping efficiency of *E. coli* in a voltage slightly higher than its critical voltage (1 V_{pp}) was observed to be less than the trapping efficiency of *C. parvum* at a voltage lower than its critical voltage (1.5 V_{pp}) [Figs. 6(b) and 6(c)]. This can be imputed to the higher $Re(f_{CM})$ of *C. parvum* at the optimal frequency as well as slightly higher applied voltage. It is noteworthy to remark that more cells were trapped at the sections away from the microchannel center attributed to lower flow velocity (as the result of parabolic flow regime) compared to the middle section. Besides, the electric field and the flow pattern were assumed to be not affected considerably due to the use of the p-DADMAC coating as it had formed a very thin layer.

D. Performance of the hybrid DEP system

A hybrid DEP system incorporated the p-DADMAC-coated surface in the DEP microfluidic system. Two aspects of the hybrid DEP system were assessed, *viz.*, quantitative evaluation of trapping efficiency of the hybrid DEP system and sustainability of the trapped cells when the electric field was switched off later. The DEP trapping experiments were conducted at the frequency of 1 MHz and at a voltage (2 V_{pp} for *E. coli* cells and 2.5 V_{pp} for *C. parvum* cells) that was low enough to clearly show the effectiveness of the hybrid DEP system. Meanwhile, the chosen voltage was slightly higher than the critical voltage, as reported earlier, to promote the pearl chaining of cells for the enhanced cell trapping. Care was taken to ensure that the chosen voltage was low enough not to saturate the electrode gaps.

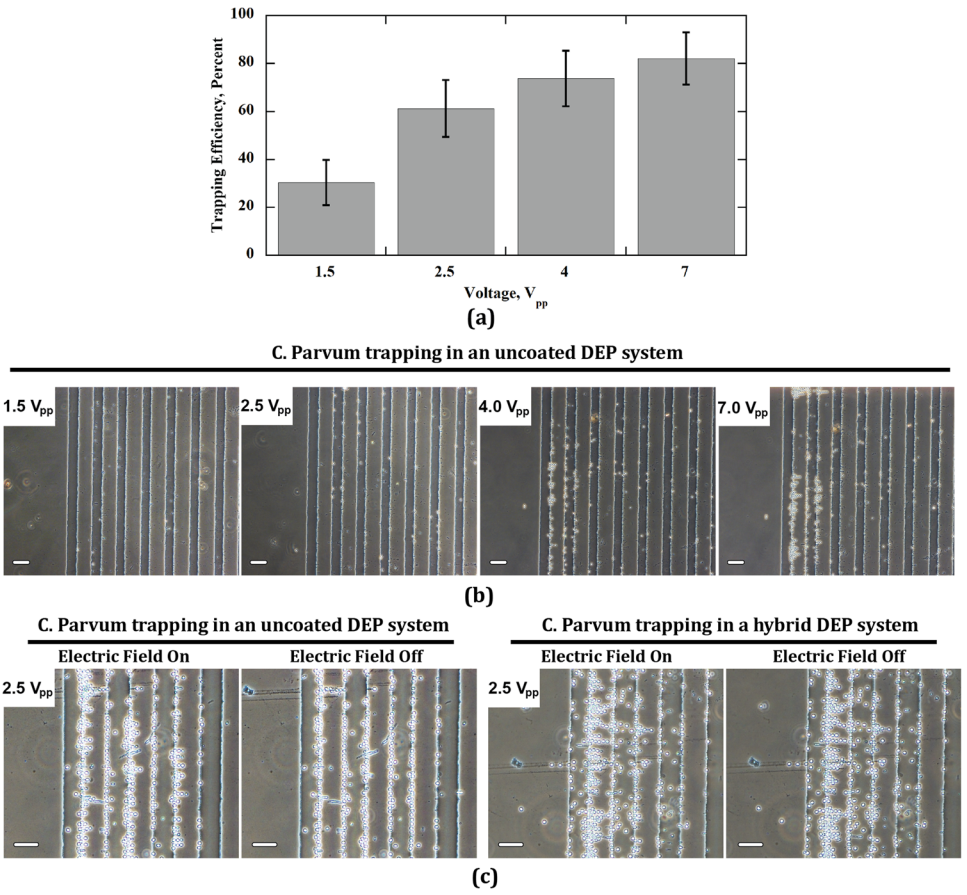

FIG. 6. (a) Change of trapping efficiency for *C. parvum* cells with respect to voltage in an uncoated DEP system and (b) its respective optical microscopic images (at $t = 30$ s). (c) Trapping of *C. parvum* cells in an uncoated and coated (hybrid) DEP system with electric field on and subsequently turning it off (at $t = 300$ s). Length of scale bars = 30 μm.

The microscopic images on the improvement of cell trapping in the hybrid DEP system as compared to the uncoated DEP system are shown in Figs. 5(c) and 6(c) for *E. coli* and *C. parvum*, respectively, and the quantitative results of this comparison are shown in Table II. The trapping efficiencies of *E. coli* and *C. parvum cells* were found to increase from 29.0% ± 1.2% and 61.3% ± 11.8% in the uncoated DEP trapping system to 51.9% ± 5.5% and 82.2% ± 1.5%, in the hybrid DEP trapping system, respectively. Thus, the hybrid DEP system was found to enhance the trapping efficiency of *E. coli* and *C. parvum* by 79% and 34%, respectively. This improvement was due to the p-DADMAC-adhesive coating in the hybrid DEP system inducing the excessive pearl-chaining formation as evident in Figs. 5(c) and 6(c). In addition, the p-DADMAC coating can aid in the trapping of those cells flowing close to the electrodes that might not otherwise trapped by p-DEP force because of the weakened electric field due to the presence of former trapped cells.

The enhancement of trapping efficiency of *C. parvum* in the hybrid DEP system (34%) was not as large as that of *E. coli*. The reason may be the difference in the cell size, which makes smaller-sized *E. coli* transport or diffusion easier than *C. parvum*. The other reason may be related to the steric repulsion of specific extra-cellular structures on *C. parvum* cell surface. In a study by Kuznar *et al.,* the presence of the macromolecules on the surface of viable *C. parvum* was identified as a limitation to the adhesion to surfaces.[37,50] These macromolecules, which include proteinaceous materials, form a brush-like structure that can result in steric repulsion once the *C. parvum* cells and surfaces initially contact.[37,50] Nonetheless, the performance of the hybrid DEP system for trapping *C. parvum* at 2.5 V_{pp} is equivalent to that of the uncoated DEP system at 7 V_{pp}, reflecting that the hybrid DEP system has equal trapping efficiency for *C. parvum* compared to the uncoated DEP system, but with application of about three times less power input. For *E. coli*, the application of the hybrid DEP system may not contribute significantly to the power-saving as a slight rise in voltage, from 2 to 2.5 V_{pp} (in an uncoated DEP system), can improve the trapping efficiency to the same extent. This can be due to more responsive trend of trapping *E. coli* to the enhancement of the applied voltage.

After switching off the electric field, the percentage of the sustained trapped cells in the system (including the first three microelectrodes) was evaluated. In the uncoated DEP system, by disrupting the electric field, there was an immediate release of cells, especially those that were involved in the formation of the pearl-like chains, since they could not sustain induced charges and the subsequent dipole-dipole interactions. About 70% of *E. coli* cells remained adhered in the hybrid DEP system when the electric field was off. In the uncoated DEP system, it was found to be only about 20%. Similarly, 97% of *C. parvum* cells remained adhered in the hybrid DEP system when the field was off. On the other hand, 75% of *C. parvum* cells was found adhered in the uncoated DEP system. These comparisons indicate the effectiveness of the p-DADMAC coating in retention of cells on the electrodes.

DEP trapping has been used to separate other contaminants from water, including microalgae and clay particles. Suscillon *et al.* have investigated the trapping of a microalgae (*Chlamydomonas reinhardtii*) in a batch mode in heterogenous media.[51] Since they employed two microelectrodes with a 2 mm wide spacing, a high voltage (40 V_{RMS}) had to be used to impart enough DEP force to reach 80% efficiency cell trapping. Conversely, our hybrid DEP system not only is capable of continuous cell trapping but also can achieve the same trapping efficiency (~80%) using much less voltage. For *C. parvum* and *E. coli* cells, 2.5 V_{pp}

TABLE II. Trapping efficiency with and without p-DADMAC surface coating at 1 MHz and 2 V_{pp} for *E. coli* and 2.5 V_{pp} for *C. parvum.*

	Trapping efficiency (%)		
	Without surface coating	With p-DADMAC coating	Percentage improvement (%)
E. coli	29.0 ± 1.2	51.9 ± 5.5	79
C. parvum	61.3 ± 11.8	82.2 ± 1.5	34

($\sim$0.9 V_{RMS}) and 5 V_{pp} ($\sim$1.8 V_{RMS}) are required to achieve the same trapping efficiency, respectively. Fatoyinbo *et al.* separated flowing clay particles (large size and mainly in the range of 10–1000 μm) from water at the flow rate of 1.02 ml/h and used a slightly larger voltage, i.e., 10 V_{pp} (3.5 V_{RMS}), as the viability was not a concern. They obtained a comparable trapping efficiency ($\sim$80%).[52] It is worthy to note that DEP trapping of large size particles/cells is easier and hence requires lower voltage ($F_{DEP} \sim r^3$). Consequently, the low applied voltage to trap smaller size cells in our case further proves the efficiency of the hybrid DEP system.

For the immune trapping of cancer cells, Huang *et al.* used a DEP-assisted capturing of three types of pancreatic cancer cells and peripheral blood mononuclear cell (all large size, 10–17 μm).[19] The cancer cells trapping was motivated by p-DEP and the peripheral cells trapping was hindered by the n-DEP impact. The $6V_{pp}$ voltage at the flow rate of 0.2 ml/h was employed. The reported capture probabilities (reported instead of capture efficiency) are between 0.05 and 0.3 for each of the cancer cells, which is lower than our reported 80% cell trapping efficiency.

The adhesion of *E. coli* and *C. parvum* on the p-DADMAC-coated surface after switching off the electric field can be explained by a widely established theory.[32,33] The adhesion of cells happens in two steps: the initial reversible attachment and then the final irreversible attachment. The first step includes the cell transport to the vicinity of the solid surface for the initial attachment. The involved forces are van der Waals forces (attractive in nature), electrostatic forces (attractive due to the opposite charges of cells and the p-DADMAC-coated surface), and hydrophobic interactions. The next step involves fixation of cell on a solid surface, for *E. coli* cells, through producing exo-polysaccharides and/or specific ligands, such as pili or fimbriae[32] and, for *C. parvum* cells, through protein-linked haltering[37] that arises in contact with a surface. To conclude, cells were pulled by a combination of forces, including p-DEP, van der Waals, and attractive electrostatic interactions, towards the close proximity of the p-DADMAC-coated surface. As a consequence, cells had sufficient time to electrostatically interact and fixate on the surface. Thus, they could endure the drag force due to fluid flow in the later absence of an electric field. The immobilized cell, after switching off the electric field, can be employed for further possible cell patterning applications or required biological testing and processing, such as on-chip Polymerase chain reaction and electrofusion.

To clean the microchannel (including microelectrodes), that is, to remove adhered cells and reuse the device, as suggested by Gómez-Suárez *et al.*, the microchannel can be washed by the air-liquid-interface detachment technique. In this technique, a series of air bubbles along with DI water were injected into the system to create a surface tension detachment force until no more improvement was observed with the subsequent washing.[53] However, the shear stress resulted from the fluid flow should be controlled to prevent the unbinding of PDMS from ITO-glass and consequently microchannel leakage. Switching the operation of the DEP microchip from p-DEP to n-DEP in conjunction with the application of high shear force can also be utilized in order to induce the detachment of the cells.[54] To work in n-DEP mode, it is recommended to change the medium to a high conductive medium such as PBS to operate in high frequency regions to prevent the microelectrodes deterioration due to the short bridging.

V. CONCLUSION

This study explored the potential application of a novel microfluidic system to separate and detect two waterborne infectious agents, *E. coli*, a bacterium and *C. parvum*, a protozoan parasite for the microbial assessment of water. A hybrid DEP system, which couples p-DADMAC-surface coating with the DEP microfluidic system, was used for the enhanced cells trapping that might otherwise be limited in an uncoated DEP system. Initial cell adhesion test on the coated glass substrate portrayed that surface charge could be a dominant factor for cell adhesion of both *E. coli* and *C. parvum*. Thus, p-DADMAC, a cationic polymer, found to be the most effective surface coating in the adhesion of both cells at the optimal coating conditions of 60 min soaking time, with 500 ppm concentration, and overnight curing at 70 °C. The optimal frequency of 1 MHz was found through characterization experiments for applying the largest

p-DEP force on both types of cells. Furthermore, it was also observed that in an uncoated DEP system, p-DEP trapping efficiencies of both cells are proportional to the applied voltage with a slightly decreasing rate of improvement at higher voltages. At a frequency of 1 MHz and 2 V_{pp} for *E. coli* cells and 2.5 V_{pp} for *C. parvum* cells, in an uncoated DEP system, the trapping efficiency of *E. coli* and *C. parvum* rose from 29.0% and 61.3% to 51.9% and 82.2% in the hybrid DEP system, respectively, due to the amplification of cell pearl-chaining. To conclude, the hybrid DEP system has shown power-saving by achieving similar efficiency as compared to the uncoated DEP system for *C. parvum* at the frequency of 1 MHz with about three times lower applied voltage (2.5 V_{pp}). On the other hand, trapping of *E. coli* in the hybrid DEP system at 2 V_{pp} exhibited comparable trapping efficiency as the uncoated DEP system at a marginally higher voltage (2.5 V_{pp}).

ACKNOWLEDGMENTS

This work was supported by research funding from the Singapore Millennium Foundation, the Singapore Ministry of Education Academic Research Fund Tier 1, and the ASTAR Nanoimprint Foundry Project No. IMRE/13-2B0278. N.A. acknowledges A*STAR for providing the SINGA scholarship for her Ph.D. The authors thank Dr. Wu Liqun for her insight about dielectrophoresis experiments and help in microfabrication, and Dr. Ma Ying for useful discussion about surface coatings. Finally, the authors would like to thank Dr. Swaine Chen in Genome of Institute of Singapore, A*STAR, for giving *E. coli* cells for experiments.

[1]B. C. Okeke, M. S. Thomson, and E. M. Moss, Sci. Total Environ. **409**(23), 4979–4985 (2011).
[2]J. P. Sidhu and S. G. Toze, Environ. Int. **35**(1), 187–201 (2009).
[3]D. Gossett, W. Weaver, A. Mach, S. Hur, H. Tse, W. Lee, H. Amini, and D. Di Carlo, Anal. Bioanal. Chem. **397**(8), 3249–3267 (2010).
[4]H. Pohl, *Dielectrophoresis: The Behavior of Matter in Non-uniform Electric Fields* (Cambridge University Press, Cambridge, 1978).
[5]B. H. Lapizco-Encinas, R. V. Davalos, B. A. Simmons, E. B. Cummings, and Y. Fintschenko, J. Microbiol. Methods **62**(3), 317–326 (2005).
[6]B. H. Lapizco-Encinas, B. A. Simmons, E. B. Cummings, and Y. Fintschenko, Electrophoresis **25**(10–11), 1695–1704 (2004).
[7]E. B. Cummings, Y. Fintschenko, V. R. Hill, and B. A. Simmons, U.S. Patent No. 7,811,439 (12 Oct. 2010).
[8]S. K. Srivastava, A. Gencoglu, and A. R. Minerick, Anal. Bioanal. Chem. **399**(1), 301–321 (2011).
[9]K.-S. Chow and H. Du, Sens. Actuators, A **170**(1–2), 24–31 (2011).
[10]H. Narayanan Unni, D. Hartono, L. Yue Lanry Yung, M. Mah-Lee Ng, H. Pueh Lee, B. Cheong Khoo, and K. M. Lim, Biomicrofluidics **6**(1), 12805–1280514 (2012).
[11]Y. H. Su, M. Tsegaye, W. Varhue, K. T. Liao, L. S. Abebe, J. A. Smith, R. L. Guerrant, and N. S. Swami, Analyst **139**(1), 66–73 (2014).
[12]C. Jaramillo Mdel, E. Torrents, R. Martinez-Duarte, M. J. Madou, and A. Juarez, Electrophoresis **31**(17), 2921–2928 (2010).
[13]A. K. Balasubramanian, K. A. Soni, A. Beskok, and S. D. Pillai, Lab Chip **7**(10), 1315–1321 (2007).
[14]H. Bridle, M. Kersaudy-Kerhoas, B. Miller, D. Gavriilidou, F. Katzer, E. A. Innes, and M. P. Desmulliez, Water Res. **46**(6), 1641–1661 (2012).
[15]T. M. Squires, R. J. Messinger, and S. R. Manalis, Nat. Biotechnol. **26**(4), 417–426 (2008).
[16]L. Yang, Anal. Lett. **45**(2–3), 187–201 (2012).
[17]L. Yang, Talanta **80**(2), 551–558 (2009).
[18]C. Ruan, L. Yang, and Y. Li, Anal. Chem. **74**(18), 4814–4820 (2002).
[19]C. Huang, J. P. Smith, T. N. Saha, A. D. Rhim, and B. J. Kirby, Biomicrofluidics **8**(4), 044107 (2014).
[20]C. Huang, S. M. Santana, H. Liu, N. H. Bander, B. G. Hawkins, and B. J. Kirby, Electrophoresis **34**(20–21), 2970–2979 (2013).
[21]C. Huang, H. Liu, N. H. Bander, and B. J. Kirby, Biomed. Microdevices **15**(6), 941–948 (2013).
[22]M. Hashimoto, H. Kaji, and M. Nishizawa, Biosens. Bioelectron. **24**(9), 2892–2897 (2009).
[23]H. C. van der Mei, M. Rustema-Abbing, D. E. Langworthy, D. I. Collias, M. D. Mitchell, D. W. Bjorkquist, and H. J. Busscher, Biotechnol. Bioeng. **99**(1), 165–169 (2008).
[24]X. Dai, J. Boll, M. E. Hayes, and D. E. Aston, Colloids Surf., B **34**(4), 259–263 (2004).
[25]H. J. Busscher and H. C. van der Mei, Clin. Microbiol. Rev. **19**(1), 127–141 (2006).
[26]B. Cetin and D. Li, Electrophoresis **32**(18), 2410–2427 (2011).
[27]L. Wu, L. Y. Lanry Yung, and K. M. Lim, Biomicrofluidics **6**(1), 14113–1411310 (2012).
[28]Z. R. Gagnon, Electrophoresis **32**(18), 2466–2487 (2011).
[29]S. Park, Y. Zhang, T. H. Wang, and S. Yang, Lab Chip **11**(17), 2893–2900 (2011).
[30]See supplementary material at http://dx.doi.org/10.1063/1.4922276 for (i) molecular structures of three coating agents and (ii) the optimization of effective parameters in surface coating.
[31]K. C. Marshall and J. A. Breznak, *Microbial Adhesion and Aggregation* (Springer Berlin Heidelberg, 1984).
[32]J. Palmer, S. Flint, and J. Brooks, J. Ind. Microbiol. Biotechnol. **34**(9), 577–588 (2007).

[33]M. Hermansson, Colloids Surf., B **14**(1), 105–119 (1999).
[34]S. Wang, S. Wen, M. Shen, R. Guo, X. Cao, J. Wang, and X. Shi, Int. J. Nanomed. **6**, 3449–3459 (2011).
[35]V. R. Regina, A. R. Lokanathan, J. J. Modrzynski, D. S. Sutherland, and R. L. Meyer, PLoS One **9**(8), e105033 (2014).
[36]C. Drozd and J. Schwartzbrod, Appl. Environ. Microbiol. **62**(4), 1227–1232 (1996).
[37]R. F. Considine, D. R. Dixon, and C. J. Drummond, Langmuir **16**(3), 1323–1330 (2000).
[38]M. Castellarnau, A. Errachid, C. Madrid, A. Juarez, and J. Samitier, Biophys. J. **91**(10), 3937–3945 (2006).
[39]W. A. Braff, D. Willner, P. Hugenholtz, K. Rabaey, and C. R. Buie, PLoS One **8**(10), e76751 (2013).
[40]J. D. Beck, L. Shang, B. Li, M. S. Marcus, and R. J. Hamers, Anal. Chem. **80**(10), 3757–3761 (2008).
[41]P. V. Jones, A. F. DeMichele, L. Kemp, and M. A. Hayes, Anal. Bioanal. Chem. **406**(1), 183–192 (2014).
[42]Y. Kuhnert-Paul, B. Bangoura, K. Dittmar, A. Daugschies, and R. Schmaschke, Parasitol. Res. **111**(1), 165–171 (2012).
[43]K. Khoshmanesh, S. Nahavandi, S. Baratchi, A. Mitchell, and K. Kalantar-Zadeh, Biosens. Bioelectron. **26**(5), 1800–1814 (2011).
[44]D. R. Albrecht, R. L. Sah, and S. N. Bhatia, Biophys. J. **87**(4), 2131–2147 (2004).
[45]J. Berthier and P. Silberzan, *Microfluidics for Biotechnology* (Artech House, 2010).
[46]O. E. Nicotra, A. La Magna, and S. Coffa, Appl. Phys. Lett. **93**(19), 193902 (2008).
[47]I. F. Cheng, H. C. Chang, and D. Hou, Biomicrofluidics **1**(2), 21503 (2007).
[48]N. M. Jesus-Perez and B. H. Lapizco-Encinas, Electrophoresis **32**(17), 2331–2357 (2011).
[49]R. Z. Lin, C. T. Ho, C. H. Liu, and H. Y. Chang, Biotechnol. J. **1**(9), 949–957 (2006).
[50]Z. A. Kuznar and M. Elimelech, Environ. Sci. Technol. **40**(6), 1837–1842 (2006).
[51]C. Suscillon, O. D. Velev, and V. I. Slaveykova, Biomicrofluidics **7**(2), 24109 (2013).
[52]H. O. Fatoyinbo, M. C. McDonnell, and M. P. Hughes, Biomicrofluidics **8**(4), 044115 (2014).
[53]C. Gomez-Suarez, H. J. Busscher, and H. C. van der Mei, Appl. Environ. Microbiol. **67**(6), 2531–2537 (2001).
[54]M. Javanmard, S. Emaminejad, R. W. Dutton, and R. W. Davis, Anal. Chem. **84**(3), 1432–1438 (2012).